XI International Conference on Computational Plasticity. Fundamentals and Applications
COMPLAS XI
E. Oñate and D.R.J. Owen (Eds)

PREDICTION OF STRAIN LOCALIZATION DURING SHEET METAL FORMING USING BIFURCATION ANALYSIS AND GURSON-TYPE DAMAGE - COMPLAS XI

L. Z. MANSOURI, H. CHALAL, F. ABED-MERAIM, T. BALAN

LEM3, UMR CNRS 7239
Arts et Métiers ParisTech
4, rue Augustin Fresnel, 57078 Metz Cedex 03, France
email: Lotfi-Zoher.MANSOURI-7@etudiants.ensam.eu, www.ensam.eu

Key words: Finite Elasto-Plasticity, Damage, Strain Localization, Sheet Metal Forming, Forming Limit Diagram.

Abstract. The strain localization phenomenon that may occur during sheet metal forming represents a major cause of defective parts produced in the industry. Several instability criteria have been developed in the literature to predict the occurrence of these instabilities. The proposed work aims to couple a Gurson-type model to the Rice's localization criterion. The implementation of the modeling is achieved via a user subroutine (Umat) in Abaqus/std using a Runge-Kutta explicit integration scheme. Finally, we show the effectiveness of the proposed coupling for the prediction of the formability of stretched metal sheets.

1 INTRODUCTION

Material instabilities in the form of shear bands represent one of the main phenomena that limit sheet metal formability. This instability in the plastic flow is still an issue for industry, since it is responsible for most of the defective parts after forming operations. Consequently, it is important to provide reliable and validated numerical tools able to predict the appearance of these plastic instabilities. The occurrence of localization through shear bands is often due to concentrations of deformation where damage is in excess. Thus, taking into account damage development during metal forming operations is essential to obtain reliable results.

Two main approaches for damage descriptions were developed in the literature during these last four decades. The first one is known as the continuum damage mechanics approach (Lemaitre [1]) and is based on the introduction of a damage variable that can be scalar or tonsorial describing the surface density of defects. The second approach, physically motivated by micromechanics concepts, accounts for the effect of the hydrostatic pressure on the material behavior through the void volume fraction. In this contribution, the second approach for damage will be used, i.e., the so-called Gurson-Tvergaard-Needleman model (GTN) [2-4].

In order to predict the onset of strain localization, it is necessary to couple the constitutive model with a localization criterion. Several localization criteria have been developed in the literature, which differ in their theoretical foundations. Brunet *et al.* [5] used the GTN model coupled with the Modified Maximum Force Criterion (MMFC) (Hora *et al*. [6]) to predict

forming limit curves for different steel grades. The obtained numerical results were compared to experimental data showing good agreements. Besson *et al.* [7] have coupled the Rice localization criterion with the GTN model for the prediction of ductile fracture in notched bars. It was shown that the introduction of the effective porosity (f^*) favors flat fracture under plane strain conditions. In the current work, the formability limits of metal sheets are investigated by means of the GTN-Rice modeling.

The paper is organized as follows: the main equations that govern the GTN model are first reviewed; then the expression of the acoustic tensor is derived within a finite strain framework. In the results and discussion section, we show the effectiveness of the proposed modeling for the prediction of forming limit diagrams (FLDs). Finally, some concluding remarks are drawn as well as some directions for future work.

2 PRESENTATION OF THE GTN MODEL

The GTN model originally proposed by Gurson [2] and phenomenologically extended by Tvergaard [3], Tvergaard and Needleman [4] is perhaps one of the most popular damage models for the prediction of the ductile fracture (Sànchez *et al.*, [8]). This damage model has shown its efficiency in particular for the prediction of the cup-cone fracture that usually appears during tensile tests of notched cylindrical bars. The approximate macroscopic yield criterion proposed by Gurson and driven from a limit analysis is given by the following relation:

$$\Phi = \left(\frac{\Sigma_{eq}}{\bar{\sigma}}\right)^2 + 2q_1 f^* ch\left(\frac{3}{2}\frac{q_2\Sigma_m}{\bar{\sigma}}\right) - \left(1 + q_3 f^{*2}\right) \leq 0 \tag{1}$$

where $\Sigma_{eq} = \left(3/2\boldsymbol{\Sigma}' : \boldsymbol{\Sigma}'\right)^{1/2}$ and $\Sigma_m = 1/3tr\left(\boldsymbol{\Sigma}\right)$ represent, respectively, the macroscopic equivalent stress and the macroscopic average stress. $\bar{\sigma}$ is the yield stress of the fully dense matrix, here only isotropic hardening is considered using a Swift law defined as follows:

$$\bar{\sigma} = k(\varepsilon_0 + \bar{\varepsilon}^p)^n \tag{2}$$

where k , ε_0 and n are parameters of the Swift hardening law and $\bar{\varepsilon}^p$ is the equivalent plastic strain of the matrix material. The parameters q_1, q_2 and q_3 were introduced by Tvergaard [9] in order to take into account the effect of interaction between cavities, and f^* represents the effective porosity, which will be defined hereafter. For the isotropic GTN model, the plastic part of the macroscopic strain rate $\mathbf{D}^p$ and the rate of equivalent plastic strain $\dot{\bar{\varepsilon}}^p$ are assumed to be related by the equivalent plastic work expression as follows:

$$(1-f)\bar{\sigma}\dot{\bar{\varepsilon}}^p = \boldsymbol{\Sigma} : \mathbf{D}^p \tag{3}$$

where f represents the void volume fraction and $\boldsymbol{\Sigma}$ the macroscopic Cauchy stress tensor. This relation is exact for $f=0$ and is a reasonable assumption for porous materials with low hardening exponents [9]. The plastic strain rate is defined by the normality law as follows:

$$\mathbf{D}^p = \dot{\lambda}\mathbf{V}_\Sigma \tag{4}$$

such as $\dot{\lambda}$ represents the plastic multiplier, and $\mathbf{V}_\Sigma = \partial\Phi/\partial\boldsymbol{\Sigma}$ is the flow direction tensor. By injecting relation (4) into (3), one obtains the rate of equivalent microscopic stress given by the following relation:

$$\dot{\bar{\sigma}} = \frac{d\bar{\sigma}}{d\bar{\varepsilon}^p}\dot{\bar{\varepsilon}}^p = H_{\bar{\sigma}}\frac{\boldsymbol{\Sigma}:\mathbf{V}_\Sigma}{(1-f)\bar{\sigma}}\dot{\lambda} \tag{5}$$

Before coalescence, the evolution of porosity is mainly due to two phenomena: nucleation and growth. It is thus possible to express the porosity rate as follows:

$$\dot{f} = \dot{f}_n + \dot{f}_g \tag{6}$$

where $\dot{f}_n$ and $\dot{f}_g$ represent the porosity rate due to nucleation and growth, respectively. In this work, it is considered that nucleation is strain controlled; in this case the evolution law of f_n due to particle fracture or particle-matrix debonding is given by the following relation [10]:

$$\dot{f}_n = \frac{f_N}{s_N\sqrt{2\pi}}\exp\left[-\frac{1}{2}\left(\frac{\bar{\varepsilon}^p - \varepsilon_N}{s_N}\right)^2\right]\dot{\bar{\varepsilon}}^p \tag{7}$$

where f_N represents the volume fraction of inclusions likely to nucleate, ε_N the equivalent plastic strain for which half of inclusions have nucleate and s_N the standard deviation on ε_N. The porosity rate due to growth depends strongly on the stress triaxiality and is given by the following relation [9]:

$$\dot{f}_g = (1-f)tr(\mathbf{D}^p) \tag{8}$$

The detection of the coalescence stage uses the phenomenological criterion introduced by Tvergaard and Needleman [7] by means of the effective porosity such as:

$$f^* = f_{cr} + \delta_{GTN}(f - f_{cr}) \tag{9}$$

with

$$\delta_{GTN} = \begin{cases} 1 & \text{if } f < f_{cr} \\ \dfrac{1/q_1 - f_{cr}}{f_R - f_{cr}} & \text{if } f > f_{cr} \end{cases} \tag{10}$$

where f_{cr} represents the critical porosity and f_R the void volume fraction at final fracture. Thus, when the material enters the coalescence phase, the introduction of effective porosity results in an accelerated degradation of its mechanical properties.

3 ELASTO-PLASTIC TANGENT MODULUS

In order to determine the expression of the elasto-plastic tangent modulus in the case of the GTN model, we apply the consistency condition given by the following relation:

$$\dot{\Phi} = \mathbf{V}_\Sigma : \dot{\mathbf{\Sigma}} + V_{\bar{\sigma}} \dot{\bar{\sigma}} + V_{f^*} \dot{f}^* = 0 \tag{11}$$

where $V_{\bar{\sigma}} = \partial\Phi / \partial\bar{\sigma}$ and $V_{f^*} = \partial\Phi / \partial f^*$. The terms involved in equation (11) are given by the following relations:

$$\mathbf{V}_\Sigma : \dot{\mathbf{\Sigma}} = \left[\frac{3}{\bar{\sigma}^2} \mathbf{\Sigma}' + \frac{q_1 q_2 f^*}{\bar{\sigma}} \mathrm{sh}\left(\frac{3}{2} q_2 \frac{\Sigma_m}{\bar{\sigma}} \right) \mathbf{I} \right] : \dot{\mathbf{\Sigma}} \tag{12}$$

$$V_{\bar{\sigma}} \dot{\bar{\sigma}} = -\frac{1}{\bar{\sigma}^2} \left[\frac{2\Sigma_{eq}^2}{\bar{\sigma}} + 3 q_1 q_2 f^* \Sigma_m \mathrm{sh}\left(\frac{3}{2} q_2 \frac{\Sigma_m}{\bar{\sigma}} \right) \right] H_{\bar{\sigma}} \frac{\mathbf{\Sigma} : \mathbf{V}_\Sigma}{(1-f)\bar{\sigma}} \dot{\lambda} \tag{13}$$

$$V_{f^*} \dot{f}^* = \left[2 q_1 \mathrm{ch}\left(\frac{3}{2} q_2 \frac{\Sigma_m}{\bar{\sigma}} \right) - 2 q_3 f^* \right] \dot{f}^* \tag{14}$$

Let us now introduce the hypo-elastic law, which reduces in the co-rotational (material) frame to a simple material derivative:

$$\dot{\mathbf{\Sigma}} = \mathbf{C}^e : \left(\mathbf{D} - \dot{\lambda} \mathbf{V}_\Sigma \right) = \mathbf{C}^{ep} : \mathbf{D} \tag{15}$$

where $\mathbf{C}^e$ represents the isotropic elasticity tensor, and $\mathbf{D}$ the strain rate tensor. Substituting equations (12) to (15) in the consistency condition, one can derive the expression of the plastic multiplier, which is given by the following relation:

$$\dot{\lambda} = \frac{\mathbf{V}_\Sigma : \mathbf{C}^e : \mathbf{D}}{H_\lambda} \tag{16}$$

where H_λ is a scalar variable such as:

$$H_\lambda = \mathbf{V}_\Sigma : \mathbf{C}^e : \mathbf{V}_\Sigma - \left(V_{\bar{\sigma}} H_{\bar{\sigma}} + V_{f^*} \delta_{GTN} A_n \right) \frac{\mathbf{\Sigma} : \mathbf{V}_\Sigma}{(1-f)\bar{\sigma}} - (1-f) V_{f^*} \delta_{GTN} \mathbf{V}_\Sigma : \mathbf{I} \tag{17}$$

substituting relation (16) in (15) gives the expression of the elasto-plastic tangent modulus as follows:

$$\mathbf{C}^{ep} = \mathbf{C}^e - \alpha \frac{\left(\mathbf{C}^e : \mathbf{V}_\Sigma \right) \otimes \left(\mathbf{V}_\Sigma : \mathbf{C}^e \right)}{H_\lambda} \tag{18}$$

where $\alpha = 0$ for elastic loading or unloading and $\alpha = 1$ in case of strict elasto-plastic loading.

4 INSTABILITY CRITERION

In addition to the behavior model, prediction of forming limits requires the use of an instability criterion allowing detection of the onset of localization. The instability criterion selected in this work is the Rice localization criterion [11-12], based on the singularity of the acoustic tensor. As discussed in the introduction, the coupling of the GTN model with the Rice instability criterion has been considered in the literature mainly for the prediction of ductile fracture in cylindrical bars under plane strain conditions. However, to the authors' knowledge, no attempt has been made for the prediction of FLDs within this constitutive and

material instability framework. Thus, the originality of the present work is to demonstrate the efficiency of such modeling in the prediction of forming limit diagrams. Then, the sensitivity of FLDs to the material parameters is investigated. The condition of localization, which can be derived from the Hadamard compatibility condition and the static equilibrium equation is given by the following relation:

$$\det\left(\mathbf{Q}\right) = \det\left(\boldsymbol{n}\cdot\mathbf{L}\cdot\boldsymbol{n}\right) = 0 \tag{19}$$

where $\mathbf{Q}$ represents the acoustic tensor, $\boldsymbol{n}$ the normal to the localization band and $\mathbf{L}$ the tangent modulus which relates the nominal stress tensor to the velocity gradient (see Haddag *et al.* [13]). Its expression is given by the following relation:

$$\mathbf{L} = \mathbf{C}^{ep} + \mathbf{L}_1 - \mathbf{L}_2 - \mathbf{L}_3 \tag{20}$$

where $\mathbf{L}_1$, $\mathbf{L}_2$ and $\mathbf{L}_3$ are fourth-order tensors induced by the large strain framework, and given by the following relations [13]:

$$\begin{aligned} L_{1ijkl} &= \sigma_{ij}\delta_{kl} \\ L_{2ijkl} &= \frac{1}{2}\left[\delta_{ik}\sigma_{lj} + \delta_{il}\sigma_{kj}\right] \\ L_{3ijkl} &= \frac{1}{2}\left[\sigma_{ik}\delta_{lj} - \sigma_{il}\delta_{jk}\right] \end{aligned} \tag{21}$$

The implementation of the above-described behavior model is carried out via a user material routine UMAT in Abaqus/standard, by means of a Runge-Kutta explicit integration scheme. This time integration scheme offers a reasonable compromise between simplicity and computational efficiency. Another reason behind the choice of an explicit scheme is that localization occurs in the softening range, and often at small stress values where implicit integration schemes (Aravas [14]) may experience difficulties at this stage of the analysis. Indeed, in the softening regime, positive definiteness of the consistent tangent modulus might not be guaranteed by classical implicit schemes (Oliver *et al.*, [15], Sànchez *et al.*, [8]). Because our main objective in this work is to show the effectiveness of the proposed framework in predicting forming limit diagrams of sheet metals, the choice of the Runge-Kutta time integration scheme is justified, despite the relatively higher computation times compared to implicit algorithms.

5 RESULTS AND DISCUSSION

In what precedes, the coupling of the GTN model with the Rice localization criterion was described. In this section, some results obtained by means of this coupling are shown. The material studied corresponds to a mild steel, mainly because of its widespread use in industry. The parameters related to this material were drawn from literature (see Brunet *et al.* [5]) and are reported in the following tables:

Table 1: Mechanical properties and strain hardening parameters

Material	E (MPa)	ν	k (MPa)	ε_0	n

Mild steel	198000	0.3	551.1	$9.54\ 10^{-3}$	0.279

Table 2: Parameters of the damage model

Material	f_0	s_N	ε_N	f_N	f_{cr}	f_R	q_1	q_2	q_3
Mild steel	10^{-3}	0.1	0.21	0.039	0.03	0.15	1.52	1.0	2.15

Figure 1-a represents the evolution of the Cauchy stress versus the true strain up to the localization point for three strain paths, namely uniaxial tension (UT), plane strain tension (PST) and balanced biaxial tension (BBT). In the case of PST, localization occurs very early, as soon as the stress-strain curve starts to soften, whereas for the BBT loading path, localization occurs for very low stress values at the end of coalescence.

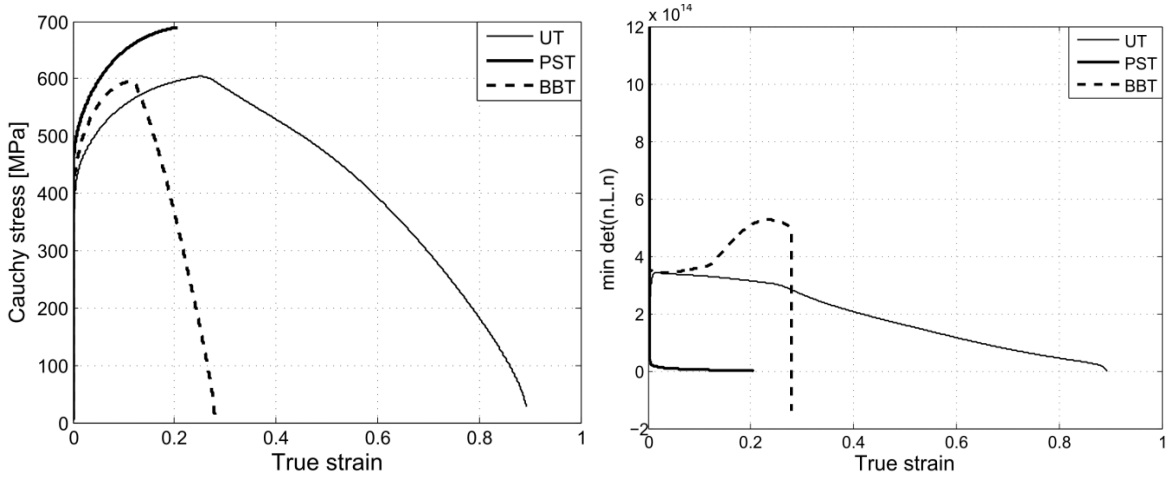

(a) (b)

Figure 1: (a) Simulation of three loading paths up to localization; (b) Evolution of the minimum of the determinant of the acoustic tensor as a function of the deformation.

Furthermore, localization takes place when the minimum of the determinant of the acoustic tensor is equal to zero (see equation (19)). In practice, during numerical computations this condition is not exactly met, and the value of det(**Q**) changes from positive to slightly negative (see Figure 1-b) during one loading increment (see also Besson et al. [7]).Figures 2-a to 2-d illustrate the effect of the coalescence parameters (f_{cr} and f_R) on the moment of detection of localization in BBT strain path. One can notice that decreasing parameter f_R results in an increase of δ_{GTN}, which makes it possible to detect localization in a premature way. On the other hand, increasing parameter f_{cr} will delay the mechanism of coalescence and in some way the occurrence of strain localization.

The modeling of coalescence phase is a major point when dealing with the proposed coupling. Indeed, Rudnicki and Rice [12] showed that for associative plasticity models (which

is our case); localization criterion can detect bifurcation only in the presence of softening behavior. Consequently, it is important to take into account the mechanism of coalescence.

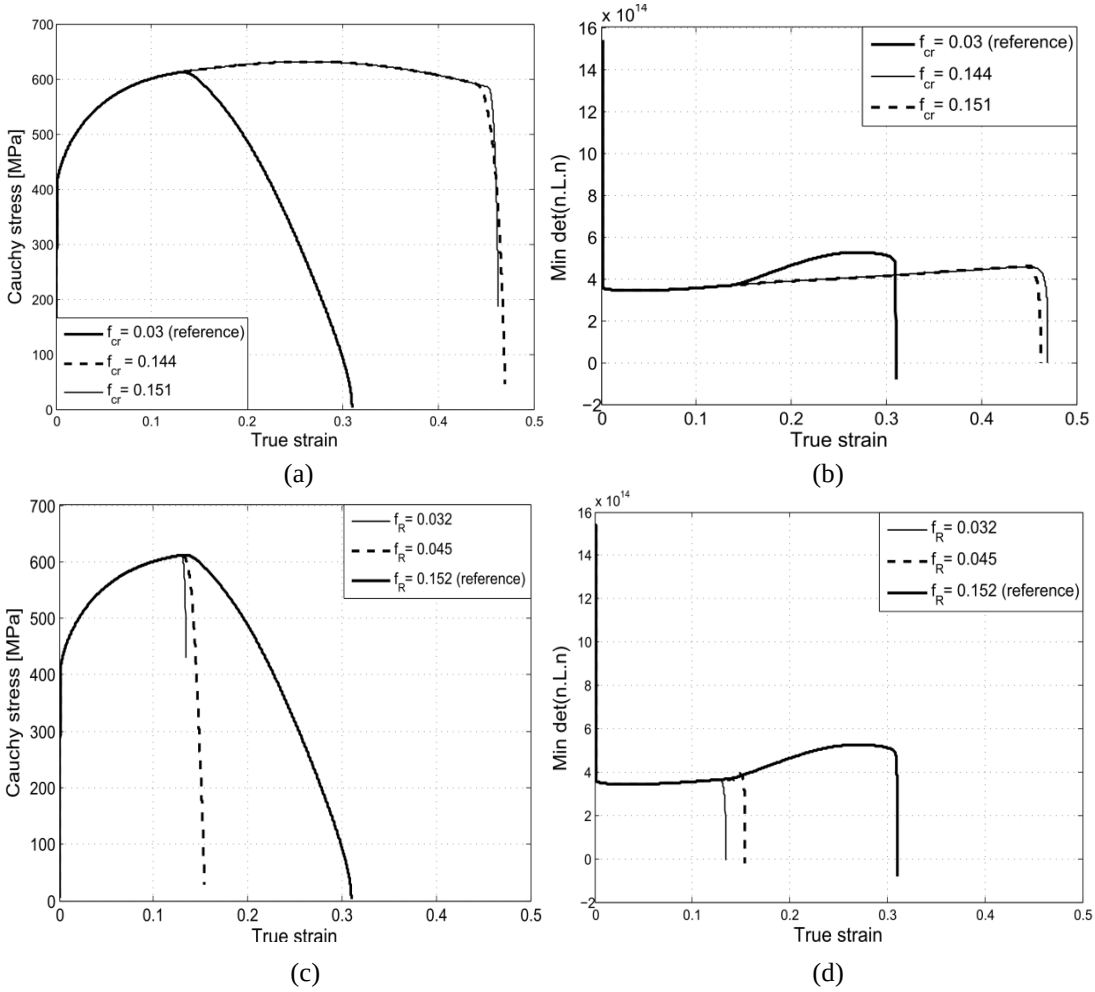

Figure 2: Effect of the coalescence parameters on the prediction of localization.

This phenomenon has a considerable effect on the obtained forming limit diagrams, since no localization can occur with the proposed modeling during positive hardening behavior. Note that several authors [16-18] suggested that parameter δ_{GTN} should not be constant, but should rather depend on other parameters, such as the stress triaxiality, initial porosity, etc. Although the coalescence model taken in the current work is kept in its simplest form (i.e., with constant parameter δ_{GTN}), the extension of this modeling framework to more physically-based descriptions can be readily done in future investigations of sheet metal formability.

5.1 Effect of the GTN parameters on the prediction of forming limits

In this section, the effect of the GTN model parameters on the prediction of FLDs is investigated. These parameters are divided into three families; each family reproducing one of the three mechanisms leading to ductile fracture (i.e. nucleation, growth and coalescence).

The results of this parametric study will be shown by varying one parameter at the same time and the reference curve will be that obtained by the parameters given in Tables 1 and 2. Thus, we will analyze the effect of initial porosity and the parameters associated with nucleation and coalescence mechanisms. Figures 4-a, 4-b and 4-c represent, respectively, the sensitivity of the FLDs to parameters f_N, s_N and ε_N.

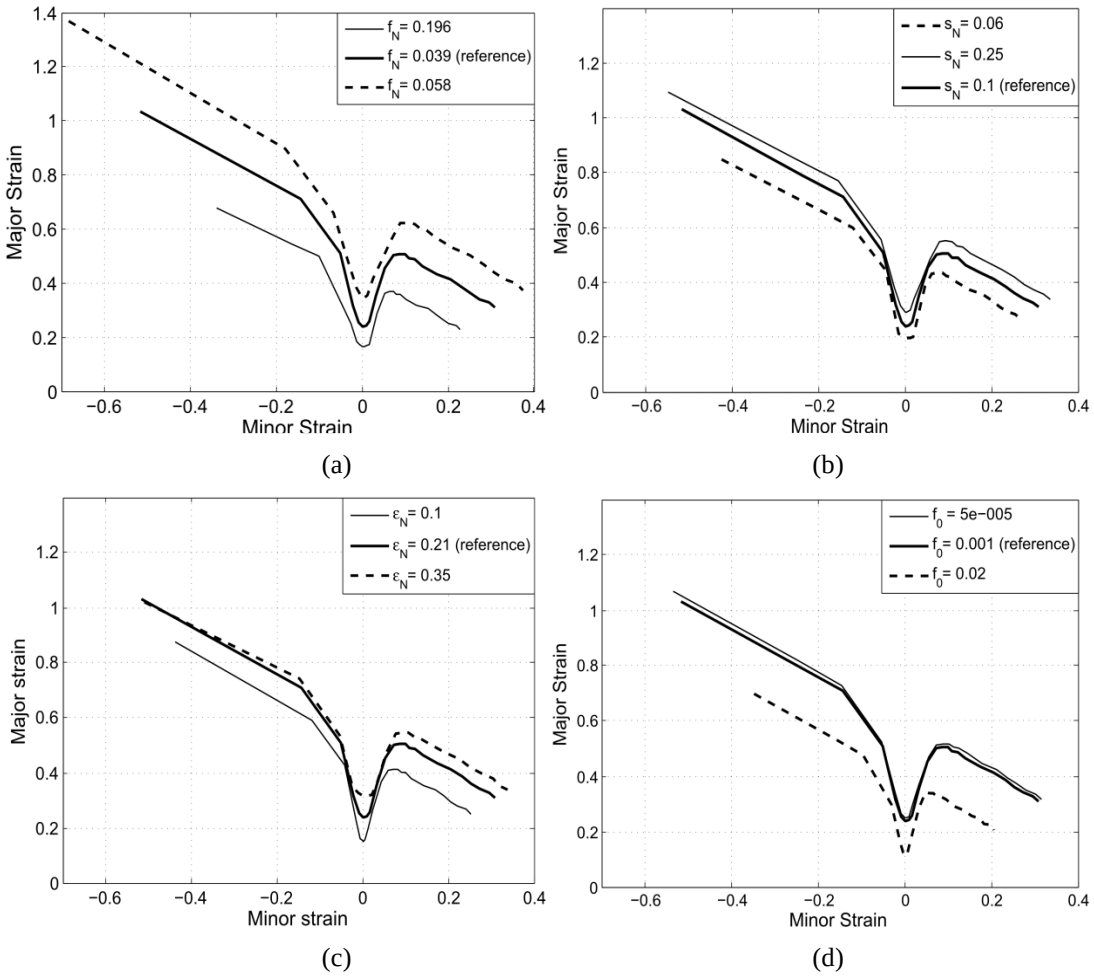

Figure 3: Effect of nucleation parameters and initial porosity on the prediction of FLDs.

The increase of f_N (decrease in s_N or ε_N) seems to have the same effect on the obtained FLD; indeed, the increase in f_N (reduction in s_N or ε_N) translates each point of the FLD downward, thus reducing the formability limits. The initial porosity is one of the most influential parameters of the GTN model, and many authors agree with its major importance (Pardoen and Hutchinson [18]). Figure 4.d represents the sensitivity of an FLD to the initial porosity; one can observe that the increase in initial porosity reduces the overall level of the FLD, and consequently reduces the material ductility.

It was shown in the previous section that the effect of coalescence parameters on the moment of occurrence of localization is crucial. In what follows, we propose to study the sensitivity of an FLD to these parameters. One notices on Figures 5-a and 5-b that variation of parameters f_{cr} and f_R strongly affects the shape of the FLDs. Indeed, this is mainly due to the role of each parameter in the coalescence modeling, since f_{cr} indicates the onset of coalescence, whereas f_R indicates the complete loss of carrying capacity.

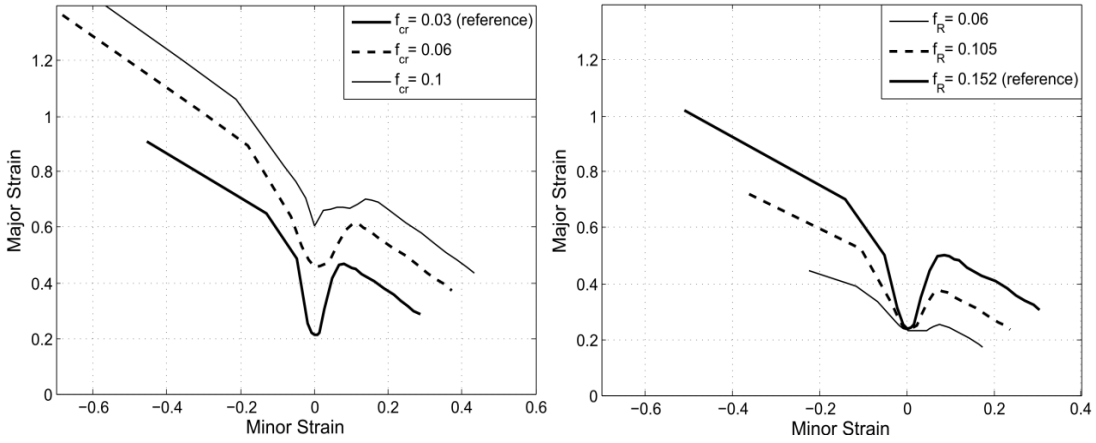

(a) (b)

Figure 4: Effect of coalescence parameters on the prediction of FLDs.

6 CONCLUSIONS

In this work, the combination of the GTN damage model and the Rice's localization criterion, which is based on the singularity of the acoustic tensor, has been proposed for application to sheet metal forming. A preliminary parametric study was conducted for different loading paths, which leads to the following observations: Concerning the nucleation parameters, it seems that the increase of f_N (decrease in s_N or ε_N) tends to lower each point of the forming limit curve. An increase of δ_{GTN} parameter accentuates the softening slope during the coalescence stage, which leads to an earlier detection of localization. It was shown that the choice of the coalescence parameters is particularly crucial in the prediction of localization. For the coalescence parameters, the increase of f_{cr} produces an upward translation of the FLD, while for f_R we notice that its decrease will lower the overall level of the FLDs.

REFERENCES

[1] Lemaitre, J.. A course on damage mechanics. (1992).

[2] Gurson, A.L.. Continuum theory of ductile rupture by void nucleation and growth: Part I-yield criteria and flow rules for porous ductile media. *Journal of Engineering Materials and Technology*, **99**(1):2–15, (1977).

[3] Tvergaard, V. Influence of voids on shear bands instabilities under plain strain conditions. *International Journal of Fracture* (1981) **32**:57-169.

[4] Tvergaard, V. and Needleman, A.. Analysis of the cup-cone fracture in a round tensile bar. *Acta Metallurgica*, (1984) **32**:57.
[5] Brunet, M., Mguil, S. and Morestin, F.. Analytical and experimental studies of necking in sheet metal forming processes. *Journal of Material Processing Technology*, (1998) **80-81**:40-46.
[6] Hora, P., Tong, L. and Reissner, J.. A prediction method of ductile sheet metal faillure in FE simulation. *Numisheet* (1996) 252-256.
[7] Besson, J., Steglich, D. and Brocks, W.. Modeling of crack growth in round bars and plane strain specimens. *International Journal of Solids and Structures* (2001) **38**:8259-8284.
[8] Sànchez, P. J., Huespe, A. E. and Oliver, J.. On some topics for the numerical simulation of ductile fracture. *International Journal of Plasticity* (2008) 24:1008-1038.
[9] Tvergaard, V.. Effect of yield surface curvature and void nucleation on plastic flow localization. *Journal of the Mechanics and Physics of Solids* (1987) **35**:43-60 .
[10] Chu, C. C. and Needleman, A.. Void nucleation effects in biaxially stretched sheets. *Journal of Engineering Material and Technology* (1980) 102:249.
[11] Rice, J. R.. The localization of plastic deformation. *Theorical and applied mechanics. Koiter ed.* (1976) 207-227.
[12] Rudnicki, J. W. and Rice, J. R. Conditions for the localization of deformation in pressure sensitive dilatant materials. *Journal of the Mechanics and Physics of Solids* (1975) **23**:71-394.
[13] Haddag, B., Abed-Meraim, F. and Balan, T.. Strain localization analysis using a large deformation anisotropic elastic-plastic model coupled with damage. *International journal of Plasticity* (2009) **25**:1970-1996.
[14] Aravas, N.. On the numerical integration of a class of pressure dependant plasticity models. *International Journal of Numerical Methods* (1987) 1395-1416.
[15] Oliver, J., Huespe, A., Blanco, S. and Linero, D. Stability and robustness issues in numerical modeling of material faillure with stong discontinuty approach. *Computer Methods in Applied Mechanical Engineering* (2005) **195:**7093-7114.
[16] Benzerga, A. A.. Micromechanics of coalescence in ductile fracture. *Journal of the Mechanics and Physics of Solids* (2002) 1331-1362.
[17] Zhang, Z. L., Thaulow, C. and Ødegård, J. A complete Gurson model approach for ductile fracture. *Engineering Fracture Mechanics* (2000) 155-168.
[18] Pardoen, T. and & Hutchinson, J. W. An extended model for void growth and coalescence. *Journal of the Mechanics and Physics of Solids* (2000) 2467–2512.